

Spatial Wilson loop in continuum, deconfining SU(2) Yang-Mills thermodynamics

Josef Ludescher*, Jochen Keller*, Francesco Giacosa†, and
Ralf Hofmann*

* *Institut für Theoretische Physik
Universität Heidelberg
Philosophenweg 16
69120 Heidelberg, Germany*

† *Institut für Theoretische Physik
Universität Frankfurt
Johann Wolfgang Goethe - Universität
Max von Laue-Str. 1
60438 Frankfurt, Germany*

Abstract

The uniqueness of the effective actions describing 4D SU(2) and SU(3) continuum, infinite-volume Yang-Mills thermodynamics in their deconfining and preconfining phases is made explicit. Subsequently, the spatial string tension is computed in the approach proposed by Korthals-Altes. This SU(2) calculation is based on a particular, effective two-loop correction to the pressure needed for the extraction of the hypothetical number density of isolated and screened magnetic monopoles or antimonopoles in the deconfining phase. By exponentiating the exchange of the tree-level massless but one-loop dressed mode within a quadratic spatial contour of side-length L in the effective theory we demonstrate that for $L \rightarrow \infty$ the Wilson loop exhibits *perimeter* law. This is in contrast to a rigorous *lattice* result subject to the Wilson action and for this action valid at sufficiently high temperature. In the framework of the effective theory there is, however, a regime for small (spatially unresolved) L where the exponent of the spatial Wilson loop possesses curvature as a function of L .

1 Introduction

In the past the pursuit of a nonperturbative understanding of 4D Yang-Mills theory at high temperature was limited to lattice formulations. A prominent target of lattice investigations is the spatial Wilson loop evaluated on a rectangular and planar contour C . Based on an analogy to the strong-coupling expansion, whose validity is suggested at sufficiently high temperature by the part of the Wilson action containing purely spacelike plaquettes, it was shown in [1] that at a given, finite, spatial lattice spacing the spatial Wilson loop always exhibits area law implying the existence of a spatial string tension σ_s . For the gauge group $SU(2)$, which we will mainly be concerned with here, this result was verified subsequently by direct simulation [2, 3, 4].

As already pointed out in [2] the argument made in [1] neither has much to say about the cutoff dependence of σ_s in the ultraviolet nor about the behavior of σ_s in the infinite-volume limit since it inherently relies on a finite spatial discretization allowing, at leading order in the strong-‘coupling’-expansion, to tile the minimal area spanned by C in terms of spacelike plaquettes. This then implies the area law in the lattice formulation.

In contrast to lattice formulations, the nonperturbative approach to $SU(2)$ and $SU(3)$ Yang-Mills thermodynamics developed in [5, 6, 7, 8] uniquely derives an effective theory for the deconfining phase starting from a genuine spacetime continuum, space being infinitely extended, and from the fundamental (euclidean) Yang-Mills action S_{YM} . The effective theory emerges as a consequence of pursuing the following chain of steps: 1) Consider the BPS saturated (topologically nontrivial) sector of (periodic) euclidean field configurations (time variable imaginary). Independent of their topological charge these (anti)selfdual configurations possess vanishing energy-stress. This implies that 2) whatever effective field is obtained as a consequence of performing a spatial coarse graining over them it is *nonpropagating*. But a nonpropagating effective field acts as a static background. 3) Such a background configuration would break the spatial isotropy and/or homogeneity of the thermal system (one-point functions) unless it is a scalar field. That is, no Lorentz tensor of rank greater than zero may emerge as an effective field from the sector of fundamental BPS saturated field configurations. If this effective scalar would be neutral under the gauge group then it would not participate in the thermodynamics due to its decoupling from the $Q = 0$ sector of propagating field configurations and its vanishing effective energy-stress. 4) Since this scalar field does not propagate its classical equation of motion is, in a given gauge, solely determined by the euclidean time dependence of its phase. 5) It turns out [9, 8] that only a single nonlocal definition of this time dependence, involving an adjointly transforming two-point function of the fundamental field strength, is possible. 6) This definition only admits the contribution of configurations with topological charge modulus $|Q| = 1$ (Harrington-Shepard (anti)calorons, trivial holonomy) because of too many dimensionful parameters spanning the moduli spaces¹ of higher-charge calorons and the instability of (anti)calorons of nontrivial holonomy [22, 12]. 7) Consistency of the thus derived second-order equation and the effective BPS saturation (first-order equation) of the adjoint scalar field uniquely fixes its gauge invariant potential with the Yang-Mills scale Λ entering as a (non-perturbative) integration constant [6, 8]. 8) Since no field other than the inert adjoint scalar may emerge from the sector(s) of BPS saturated fundamental field configurations the coupling to the sector of propagating gauge fields ($Q = 0$), which by perturbative renormalizability [17] by itself cannot generate higher dimensional operators upon the invoked spatial coarse-graining, occurs minimally via the square of the adjoint covariant derivative, see also Sec.2. 9) The thus derived effective action yields an accurate a priori estimate for the thermal ground state by solving the Yang-Mills equation of the effective $Q = 0$ sector in the background of the adjoint scalar field. 10) Radiative corrections to the free quasiparticle situation described by the effective action can be integrated out in a rapidly converging loop expansion subject to constraints imposed by the

¹Due to the temperature independence of the weight $e^{8\pi^2|Q|/g^2}$ (g the fundamental, classical and thus temperature independent coupling *constant*) the definition of the time dependence of the field’s phase must not invoke any explicit temperature dependence. This only leaves room for the spatial coarse-graining over a two-point function of the fundamental field strength.

existence of an effective thermal ground state [7]. Interestingly, only planar bubble diagrams contribute. As we will see, the maximal resolution of the effective theory, which is given by the scalar field's modulus, almost everywhere in temperature is too small to allow for the existence and dynamics of single magnetic monopoles and antimonopoles, generated by (anti)caloron deformation away from trivial holonomy and away from BPS saturation, to be resolved.

We consider it useful to repeat the above steps including physical interpretations. A sufficiently local spatial coarse-graining [9] over stable and absolute minima of the action in the sector with topological charge modulus $|Q| = 1$ (Harrington-Shepard (anti)calorons [10], nonpropagating configurations) generates a spatially homogeneous and inert adjoint scalar field ϕ whose modulus sets the maximally available resolution in the effective theory². Recall, that only this sector is allowed to contribute to the kernel containing ϕ 's phase [5, 8, 9]. The inertness of the field ϕ and the spatial homogeneity of its (gauge-invariant) modulus derives from the fact that it is obtained as a spatial average over nonpropagating, stable BPS saturated (zero energy-stress) field configurations³. This can be checked explicitly by computing the curvature of ϕ 's potential and by comparing it with the squares of maximal resolution $|\phi|$ in the effective theory and T [5]. So the effect of performing the spatial coarse graining over Harrington-Shepard (anti)calorons is to make explicit the spatial homogeneity and isotropy of the thermal system as contributed to by the only topologically non-trivial gauge-field configurations which are admissible in computing a useful a priori estimate of the thermal ground state. The average effect of domainizations of the field ϕ , which necessarily would lead to the emergence⁴ of spatially localized and isolated magnetic charges [13], is accounted for by the quantum field theoretic method of loop expansion [7, 14, 15, 16]. Again, to each order of this expansion, spatial isotropy and homogeneity are granted features. The sector with $Q = 0$ and its coupling to the inert field ϕ after spatial coarse-graining is uniquely determined by perturbative renormalizability [17], gauge invariance, and the spacetime symmetries of the underlying theory, for an explicit presentation see Sec. 2.

Apart from 1-PI reducible diagrams for the polarization tensor, which as compared to the tree-level situation can be resummed into mildly modified dispersion laws, the expansion into irreducible loop diagrams is expected to terminate at a finite loop order [7]. Numerically, there is a large hierarchy between leading, next-to-leading, and next-to-next-to-leading corrections to the pressure [14, 15]. As far as propagating, effective gauge modes are concerned, this is the reason why essentially all physics is contained in the tree-level quasi-particle spectrum and the resummed, one-loop polarization [14, 15, 18].

Interactions between two topologically distinct sectors are hard to grasp when working with fundamental fields. As it turns out, in a situation determined by a global temperature scale T (infinite-volume thermodynamics) the explicit consideration of fundamental fields and their interactions would necessitate external probes whose resolution needed to exceed the value $|\phi|$ emerging in terms of the Yang-Mills scale Λ and T when (sufficiently locally) integrating out the sector with $|Q| = 1$. That is, an attempt to saturate the partition function in terms of fundamental field configurations, resolved with a higher momentum transfer than $|\phi|$, necessarily introduces unsurmountable complications in assuring that the according approximations sustain homogeneous and isotropic thermalization.

The main purpose of the present work is to investigate the physics of screened magnetic charges,

²A nontrivial-holonomy (anti)caloron [11] is not stable. Moreover, it is suggested to consider a slow dependence in real time of the holonomy parameter u since a constancy of u in space and time would completely suppress the weight of the nontrivial-holonomy caloron in the thermodynamic limit [12]. This time dependence, however, necessarily lifts the associated field configuration above the BPS bound. On the level of the effective theory, where the thermal ground state is described by the field ϕ together with a pure-gauge configuration of the coarse-grained $Q = 0$ sector, this microscopic lift above the BPS bound is seen in terms a positive ground-state energy density which is the negative of its pressure [5, 8].

³Inertness of ϕ follows from the fact that a spatial average over nonpropagating fields can not generate propagating modes in the effective field ϕ . Thus an inhomogeneity of $|\phi|$ would explicitly break the homogeneity of one-point functions which is in contradiction to infinite-volume continuum thermodynamics.

⁴Microscopically, the emergence of these charges is understood by the dissociation of large-holonomy, that is, strongly-deformed-away-from-the-Harrington-Shepard-situation (anti)calorons.

being held responsible for the emergence of an area law for the spatial Wilson loop at high temperatures in lattice gauge theory. We perform the analysis both in a hypothetical microscopic fashion and by directly appealing to the effective theory. As a warm-up to the effective theory for the deconfining phase we start by showing the uniqueness of the effective action in Sec. 2. In Sec. 3 we review the argument given by Korthals-Altes for the existence of a spatial string tension as originated by isolated, screened and statistically independent magnetic charges. This argument assumes (anti)monopoles to behave like classical (resolvable) particles which, due to sufficiently strong screening, separately contribute their magnetic flux through the minimal surface spanned by the spatial contour. In Sec. 4 we use a two-loop correction to the pressure, calculated in the effective theory and surviving the high-temperature limit, to extract the average mass of the screened and stable monopole-antimonopole system. Subsequently, their hypothetical⁵ number density n is determined. As an aside, we demonstrate that, despite the hypothetical screening length being about three times larger than the intermonopole distance in an *ensemble* of, isolated, stable and screened (anti)monopoles there is no large effect on their mass when comparing with the BPS mass of an *isolated* monopole-antimonopole pair immersed into a sea of instable dipoles. The hypothetical number density n in turn would imply a spatial string tension if the potentials of these stable magnetic (anti)monopoles would not overlap such as to cancel their magnetic flux. Recall that the derivation of an area law, as performed in [19], relies on a counting argument for Poisson distributed (anti)monopoles. This argument assumes the independence of individual (anti)monopoles contributing to the total magnetic flux through a given spatial surface. This independence, however, turns out to be strongly violated because stable magnetic objects essentially cancel their fluxes locally through their overlapping magnetic potentials. The immediate implication then is that the spatial Wilson loop cannot exhibit area-law behavior at high temperatures. We confirm this result in Sec. 5 where the spatial Wilson loop is computed involving the lowest nontrivial radiative corrections for the dispersion law of the massless mode in the effective theory: A resummation of the one-loop polarization of the massless mode both on- and off-shell. In computing the spatial Wilson loop in real time we take into account the quantum and the thermal parts of the modified propagator for the massless mode, and we discuss the potential contribution of the massive modes. We also consider the magnetic screening mass, defined as the zero-momentum limit of the square root of the screening function when setting the temporal component of the momentum equal to zero (Secs. 5.1 and 5.5). In Sec. 6 we summarize our work and conclude.

2 Only minimal coupling of $Q = 0$ with $|Q| = 1$ sector in the effective action for the deconfining phase

Here we would like to argue that the effective action of the deconfining phase

$$S_{\text{dec}} = \text{tr} \int d^4x \left\{ \frac{1}{2} G_{\mu\nu} G_{\mu\nu} + D_\mu \phi D_\mu \phi + \frac{\Lambda^6}{\phi^2} \right\}. \quad (1)$$

is complete. Namely, no operators representing local vertices of the field a_μ with three or more external legs together with (powers of) the field ϕ are possible while the nonexistence of operators of mass dimension larger than four *solely* involving the gauge field a_μ is excluded by perturbative renormalizability [17]. Notice that nonlocal contributions to the effective action always can be expanded in powers of covariant derivatives.

⁵By hypothetical we mean a physical number density seen by applying a sufficiently large spatial resolution a^{-1} to typical configurations thermalized according to an associated perfect lattice action. The latter is constructed such that the full partition function of the theory is invariant under a change $a \rightarrow a'$. Due to an efficient magnetic-charge neutralization it will turn out that this number density appears to be zero when applying the low resolution $|\phi|$ of our effective theory. The practical advantage of the low resolution $|\phi|$ is that it renders the perfect action to be extremely simple and thus useful: The assumptions of ?? about screened magnetic monopoles and antimonopoles contributing their magnetic flux essentially uncanceled through the minimal contour spanning the spatial loop can be quantitatively checked by comparing screening length with mean spatial separation.

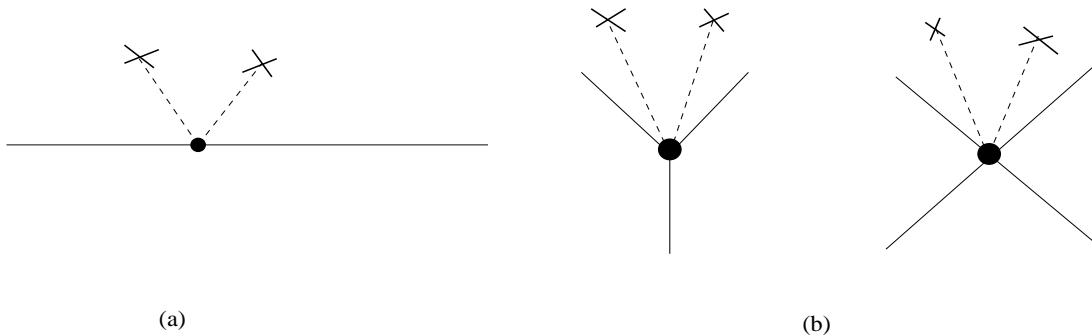


Figure 1: Allowed vertex (a) and examples of lowest mass dimension for excluded vertices in the effective theory (b). Solid lines represent the topologically trivial gauge field a_μ while a dashed line terminating in a cross corresponds to a local insertion of the operator ϕ .

Examples for excluded operators, still allowed by the spacetime symmetries and gauge invariance, would be

$$\text{tr} \frac{1}{M^{2(3n-2)}} (G_{\mu\nu}[D_\mu\phi, D_\nu\phi])^n, \quad (n \geq 1), \quad (2)$$

M representing some mass scale, while the operator $\text{tr} D_\mu\phi D_\mu\phi$ appearing in the action of Eq. (1) is allowed. Fig. 1 depicts the situation of the allowed operator $\text{tr} D_\mu\phi D_\mu\phi$ and the $n = 1$ operator of (2), which suffices to state our argument diagrammatically. Field ϕ is energy and pressure free. (Its existence is owed to $|Q| = 1$ (anti)selfdual fundamental configurations of trivial holonomy.) Assuming a local vertex of ϕ with more than three external legs (in consistency with gauge invariance and spacetime symmetries) coming from the gauge fields of the coarse-grained trivial-topology sector a_μ necessarily would imply momentum transfer to the field ϕ , see (b) of Fig. 1 for a lowest-dimension example. That is, the probability of not transferring momentum to ϕ for non-vanishing momenta associated with the external legs of field a_μ is zero since this situation would correspond to a hypersurface in the space of all possible momentum transfers. But a transfer of energy-momentum to ϕ would change its own energy-momentum to nonvanishing values. This, however, contradicts ϕ 's BPS property. For the vertex of ϕ with two external legs of the field a_μ (mass term in unitary gauge), as it is represented by the term $\text{tr} (D_\mu\phi)^2$ in the effective action of Eq. (1) and depicted in (a) of Fig. 1, no momentum is transferred. (Massiveness of the off-Cartan topologically trivial gauge field a_μ emerges only after an infinite resummation of such a vertex.) The fact that the ground state as such has a finite energy density in the effective theory is owed to a pure gauge configuration. This configuration on the effective level sums up interactions (energy-momentum transfers *larger* than $|\phi|$, that is at distances smaller than $|\phi|^{-1}$) of topologically trivial fundamental gauge fields with (anti)calorons which are not visible at resolution lower than $|\phi|$ but lift the ground-state energy density from zero to a finite value (temporary shift of holonomy plus radiative corrections).

To conclude, the existence of vertices involving ϕ and more than two legs of the coarse-grained topologically trivial gauge field a_μ in the effective theory for the deconfining phase is excluded by the BPS property of ϕ : The very existence of ϕ , which is guaranteed to emerge from the $|Q| = 1$ sector of the theory upon spatial coarse-graining [9, 5, 8], would be contradicted by it absorbing energy-momentum *after* coarse-graining.

As for the preconfining phase, renormalizability is trivial since we coarse-grain over the non-interacting $Q = 0$ sector of a $U(1)$ (or $U(1)^2$ in the case $SU(3)$) gauge theory. Thus the same arguments as for the deconfining phase when adjusted to this simpler, abelian situation do fix the action of the associated Higgs model [5] uniquely in the preconfining phase.

3 Korthals-Altes' derivation of fundamental spatial string tension

We only consider the case of deconfining SU(2) Yang-Mills thermodynamics with Yang-Mills scale Λ . In the effective theory for this phase the tree-level situation is described by an inert adjoint and spatially homogeneous scalar field of modulus $|\phi| = \sqrt{\frac{\Lambda^3}{2\pi T^3}}$, a pure-gauge configuration of the coarse-grained $Q = 0$ sector, and propagating gauge modes (one direction of the SU(2) algebra massless, two directions of mass $2e|\phi|$). This effective theory neatly decomposes physics into a thermal ground state (equation of state equal to that of a cosmological constant but with a temperature dependent energy density) and thermally fluctuating (quasi)particles⁶. Notice that on tree-level this 'a-priori-estimate' for the thermal ground state only captures the physics of small-holonomy (anti)calorons which are associated with short-lived monopole-antimonopole pairs. This leads to an explicit manifestation of spatial homogeneity and isotropy in terms of ϕ and a pure gauge a_μ^{gs} as it is demanded by thermodynamics. The effects attributed to the rare occurrence of isolated, long-lived, and screened magnetic charges in the plasma are captured by certain radiative corrections. This can be pictured as an implicit average over domainized ϕ -field configurations [13] of typical domain size smaller than $|\phi|^{-1}$ facilitated by the quantum field theoretic method of loop expansion in effective variables. Notice that spatial homogeneity and isotropy are explicitly honored at each loop order.

Before we actually establish the connection between radiative corrections to the pressure as computed in the effective theory and the hypothetical physics of screened magnetic monopoles we would like to review the arguments given by Korthals-Altes [20] on how a spatial string tension emerges once the existence and independence of isolated and screened (magnetic screening length l_s) magnetic charges is assumed in the plasma. Korthals-Altes considers a quadratic, spatial contour of side-length L and a number density of monopoles n_M . Since monopoles are created pairwise by the dissociation of large-holonomy calorons⁷ one has $n_M = n_A \equiv n$ where n_A is the number density of antimonopoles. Furthermore, he assumes (and justifies this assumption by lattice data obtained with the Wilson action) that monopoles and antimonopoles fluctuate in an independent way and that they are rare. This is certainly true if the screening length l_s is much smaller than the mean interparticle distance $d = (\frac{1}{n})^{1/3}$. We will show in Sec. 4.2, however, that this situation is actually *not* realized. Still, the mass of the screened monopole-antimonopole system is close to its BPS bound.

By virtue of the length scale l_s Korthals-Altes considers a slab of thickness $2l_s$ containing magnetic quasiparticles. These quasiparticles contribute a mean magnetic flux through the minimal surface spanned by the afore-mentioned contour. Only those quasiparticle that are contained within the slab are held responsible for the flux. A more refined treatment introducing no such constraint but taking into account a Yukawa-like potential for the static magnetic field sourced by each of these objects yields similar results.

As a brief interlude, we name an important property of these monopole-antimonopole pairs. Since we know now that pairs of magnetic monopoles and antimonopoles are liberated through the dissociation of large-holonomy (anti)calorons we also know – by studying the BPS (anti)monopole constituents in such (anti)calorons [11] – that the combined mass $m \equiv m_M + m_A$ of the monopole

⁶Due to the existence of the maximal resolution scale $|\phi|$ the effect of having coarse-grained gauge modes propagate off their mass shell without explicit interaction is, on the one-loop level, completely negligible for thermodynamical quantities such as the pressure [5].

⁷Notice that the occurrence of a nontrivial caloron holonomy in the sense of a spacetime independent parameter, as it occurs in (anti)selfdual Yang-Mills fields, is unphysical because of the vanishing impact of these configurations onto the partition function [12]. In case of small holonomy it is still useful though to think of the holonomy parameter as possessing a finite-support real-time dependence of width that is comparable to the life-time of the monopole-antimonopole pair. Upon a continuation of this real-time dependence back to the euclidean a departure from (anti)selfduality takes place.

and its antimonopole (a holonomy-independent quantity) is roughly given as [11]

$$m \sim \frac{8\pi^2 T}{e} = \sqrt{8}\pi T \sim 8.89 T. \quad (3)$$

Here the high-temperature plateau-value $e = \sqrt{8}\pi$ for the *effective* gauge coupling e was used [5, 8, 21]. Eq. (3) is valid for an isolated, noninteracting (test) monopole-antimonopole system with their magnetic charges being screened by the surrounding, short-lived magnetic dipoles belonging to small-holonomy (anti)calorons. This is the situation described by the one-loop expressions for thermodynamical quantities in the effective theory. By virtue of Eq. (3) magnetic monopoles and antimonopoles appear as nonrelativistic objects in the plasma. They are Boltzmann suppressed as

$$P_{M+A} \sim \exp(-\sqrt{8}\pi) \sim 1.4 \times 10^{-4}, \quad (4)$$

and thus occur rarely as compared to the instable pairs that are associated with small (anti)caloron holonomies.

Now Korthals-Altes exponentiates the normalized flux $\Phi_{l=1}$ of a single (anti)monopole through the minimal surface spanned by the contour in the limit $L \rightarrow \infty$ as

$$V(L)|_{l=1} \equiv \exp\left(2\pi i \frac{\Phi_{l=1}}{Q}\right), \quad (5)$$

where Q is the magnetic charge. Depending on the sign of Q and on the location w.r.t. the minimal surface one has $\Phi_{l=1} = \pm \frac{1}{2}$ and thus

$$V(L)|_{l=1} \equiv -1. \quad (6)$$

Korthals-Altes now assumes the probability $P(l)$ for the occurrence of l charges within the slab to be given by the Poisson distribution

$$P(l) = \frac{\bar{l}^l}{l!} \exp(-\bar{l}), \quad (7)$$

where \bar{l} is the mean value of the number of magnetic charges contained inside the slab. One then obtains

$$\bar{V}(L) = \sum_{l=0}^{\infty} P(l) (-1)^l = \exp(-2\bar{l}). \quad (8)$$

Since $\bar{l} = 4 A(L) l_s n(T)$, where $A(L)$ is the minimal surface and $n(T)$ is the (temperature-dependent) density of monopoles (or antimonopoles or monopole-antimonopole pairs), we observe that the Wilson loop shows area law with tension σ_s given as

$$\sigma_s = 8 l_s n(T). \quad (9)$$

Notice that the hypothetic magnetic screening length l_s is given in terms of n and T as [20]

$$l_s = \frac{1}{g} \sqrt{\frac{T}{n}}, \quad (10)$$

where g is the magnetic coupling: $g \equiv \frac{4\pi}{e}$.

4 Monopole physics from two-loop correction to the pressure

In this section we would like to investigate the high-temperature implications of the radiative corrections to the pressure, calculated in the effective theory, for the physics of unresolved, stable and screened magnetic monopoles and antimonopoles as they emerge from the dissociation of large-holonomy (anti)calorons. Notice that the density of these objects is inferred purely energetically without making reference to the existence or nonexistence of their net magnetic fluxes.

4.1 Mass of interacting monopole-antimonopole system

On distances larger than the minimal spatial length [5]

$$|\phi|^{-1} = \frac{(13.87)^{3/2}}{2\pi T_c} \sqrt{\frac{T}{T_c}} \quad (11)$$

and not taking into account radiatively liberated stable and isolated monopole-antimonopole pairs, the depletion of a single magnetic test charge is described by the effective, electric coupling $e = \sqrt{8}\pi$ for $T \gg T_c$. Notice that the (constant) value of e signals that for $T \gg T_c$ the system forgets about the presence of the Yang-Mills scale Λ as far as its propagating degrees of freedom are concerned: The thermodynamics of these modes then solely is determined by topology and temperature. This fact may be conceived as a nonperturbative manifestation of asymptotic freedom.

It is important to stress that the effective, electric coupling rapidly approaching the constant $e = \sqrt{8}\pi$ at increasing temperature is a consequence of an evolution equation assuring that the interaction of the thermal ground state with propagating quasiparticle excitations honours Legendre transformations [5, 8]. The constancy $e = \sqrt{8}\pi$ is approached power-like fast in T . So the error of using the constant $e = \sqrt{8}\pi$, which is a lower bound on the behavior close to the phase transition, at moderate temperatures dies off in a power-like way. In [14] we have used the exact evolution of e and, indeed, have observed, within a few percent variation, the asymptotic constancy of the two-loop correction to the pressure divided by T^4 starting from $T = 3T_c$. Asymptotic constancy of e is not to be confused with the behavior of the *fundamental* gauge coupling which can be defined via the trace anomaly of the energy-momentum tensor [21]. The latter approaches zero logarithmically slowly with increasing T .

The holonomy-independent sum m of the masses of the BPS monopole and BPS antimonopole (BPS mass), being the constituents of a nontrivial-holonomy (anti)caloron, is given as [5, 11]

$$m_{>|\phi|^{-1}} = \frac{8\pi^2 T}{e} = \sqrt{8}\pi T. \quad (12)$$

Notice that Eq. (12) describes the situation of a pair of BPS saturated monopole and antimonopole placed as test charges into a surrounding where small-holonomy (anti)calorons generate short-lived magnetic dipoles effectively leading to a finite renormalization of the magnetic charge of the test particles. Here no departure from the BPS limit is implied, and the U(1) gauge field of the test (anti)monopole still is infinite-range. A linear superposition of these potentials then leads to a dipole form which for large distances R decays like $1/R^3$. This corresponds to the approximation of a massless and two massive *free* thermal quasiparticles in the effective theory (tree-level).

On the level of radiative corrections, however, we are concerned with the physics of isolated, stable magnetic charges whose average distance $n^{-1/3}$ at high temperature will be given by $n^{-1/3} = c/T$ where c is a positive, real constant (determined in Sec. 4.2). Thus

$$|\phi| n^{-1/3} = 2\pi c \left(\frac{T_c}{13.87 T} \right)^{3/2}, \quad (13)$$

which is smaller than unity for sufficiently high T . In fact, an estimate implies that for $T \geq 1.91 T_c$ isolated and screened (anti)monopoles are not resolved in the effective theory. This estimate uses the high-temperature value $e = \sqrt{8}\pi$ for the effective gauge coupling. A more careful investigation for T shortly above T_c shows that isolated and screened (anti)monopoles actually are never fully resolved in the effective theory for the deconfining phase. However, their effect on the propagation of the tree-level massless gauge mode is sizable at temperatures a few times T_c [14, 18].

To make contact with degrees of freedom, whose collective long-distance effects are detectable (antiscreening and screening of effective gauge-field propagation) but which never appear explicitly in the effective theory, we may consider the situation of thermally fluctuating, free quasiparticles (one-loop truncation of loop expansion of the pressure) as the asymptotic starting point. Small

interactions between the quasiparticles, as they are described by radiative corrections (for $T \gg T_c$ only the two-loop diagram involving a four-vertex connecting on shell a massless with either of the two massive modes survives) introduce interesting physics but do not change the energy density of the one-loop situation. The important implication then is that radiative corrections to the one-loop situation, calculable in the effective theory, must be *cancelled* by the physics of unresolved degrees of freedom on the level of thermodynamic quantities. By the result of [22], which shows that (anti)calorons dissociate upon strong quantum deformation into isolated magnetic monopole–antimonopole pairs, we are led to conclude that these degrees of freedom are indeed isolated, stable, and screened magnetic monopoles and antimonopoles.

Thus we need to compute the mass m of monopole-antimonopole systems for distances of the order of $n^{-1/3}$. Since the spatial coarse-graining, which determines the field ϕ , saturates exponentially fast on distances of a few $\beta \equiv 1/T$ [8, 9] we expect that

$$\frac{m}{m_{>|\phi|^{-1}}} = O(1) \quad (14)$$

which, indeed, is the case. Let us show this.

As mentioned above, at large temperatures the two-loop diagram for the pressure involving a four-vertex connecting a massless with either of the two massive modes is the only surviving radiative correction [14, 23]. For $T \gg T_c$ one has [14]

$$\frac{\Delta P_{2\text{-loop}}}{P_{1\text{-loop}}} = -4.39 \times 10^{-4}, \quad (15)$$

where $\Delta P_{2\text{-loop}} \equiv P_{2\text{-loop}} - P_{1\text{-loop}}$. Since for $T \gg T_c$ we have [5]

$$P_{1\text{-loop}} = \frac{4}{45} \pi^2 T^4 \quad (16)$$

the correction $\Delta P_{2\text{-loop}}$ is also proportional to T^4 . Now $\Delta P_{2\text{-loop}}$ and the associated energy density $\Delta \rho_{2\text{-loop}}$, which both are negative, must obey the following relation⁸

$$\Delta \rho_{2\text{-loop}} = T \frac{d\Delta P_{2\text{-loop}}}{dT} - \Delta P_{2\text{-loop}}. \quad (17)$$

Eq. (17) and the fact that $\Delta P_{2\text{-loop}} \propto T^4$ imply an equation of state

$$\Delta \rho_{2\text{-loop}} = 3 \Delta P_{2\text{-loop}}, \quad (18)$$

and Eq. (15) tells us that the thermal energy density $\Delta \rho_{M+A}$, attributed to the presence of unresolved, screened, isolated pairs of (no longer BPS saturated) magnetic monopoles and antimonopoles is given as⁹

$$\begin{aligned} \frac{\Delta \rho_{M+A}}{T^4} &\equiv \frac{1}{2\pi^2} \int_{\mu}^{\infty} dy \sqrt{y^2 - \mu^2} y^2 n_B(y) \stackrel{!}{=} -\frac{\Delta \rho_{2\text{-loop}}}{T^4} \\ &= 4.39 \times 10^{-4} \times \frac{4}{15} \pi^2, \end{aligned} \quad (19)$$

where $\mu \equiv m/T$ and $n_B(y) \equiv 1/(\exp(y) - 1)$. The only positive solution μ of Eq. (19) is numerically given as $\mu = 10.1224$. Thus we have

$$\frac{m}{m_{>|\phi|^{-1}}} = 1.139. \quad (20)$$

⁸Legendre transformations are linear and thus hold for each order in the loop expansion separately when integrating out residual quantum fluctuations.

⁹Since the process of (anti)caloron dissociation, creating pairs of isolated and screened magnetic (anti)monopoles subject to an exact, overall charge neutrality, is irreversible the density of these objects is sharply fixed at a given temperature. Thus there is no chemical potential associated with monopole-antimonopole pairs.

The effect of all other, screened, isolated, and stable (anti)monopoles, generated by the dissociation of large-holonomy (anti)calorons, hence is a lift of the mass of the system by about 14% above the BPS bound even though the hypothetic magnetic screening length l_s at high T is larger than the mean interparticle distance \bar{d} , see Sec. 4.2.

4.2 Monopole density, (anti)monopole distance, and screening length

Knowing that $\mu = 10.1224$ we now can compute the hypothetic monopole density n as

$$n = \frac{T^3}{2\pi^2} \int_{\mu}^{\infty} dy y \sqrt{y^2 - \mu^2} n_B(y) = 9.799 \times 10^{-5} T^3. \quad (21)$$

For reasons of symmetry there is a *universal* mean monopole-antimonopole distance \bar{d} . That is, the distance between a monopole and its antimonopole, both stemming from the dissociation of the same (anti)caloron, is, on average, the same as the distance between a monopole adjacent to an antimonopole who did not originate from the same (anti)caloron. From Eq. (21) we have

$$\bar{d} = n^{-1/3} = 21.691 \beta. \quad (22)$$

Thus the constant c in Eq. (13) is given as $c = 21.691$, and the right-hand side of (13) is smaller than unity for $T > 2T_c$. That is, isolated and screened (anti)monopoles are *not resolved* at high temperatures in the effective theory. Because the magnetic flux of a given pair essentially cancels due to the large overlap of magnetic potentials no area law is to take place for the spatial Wilson loop, see Eq. (24). This is in accord with our investigation performed in Sec. 5.

By virtue of Eqs. (23) and (21) the hypothetic magnetic screening length l_s is given as

$$l_s = \frac{1}{g} \sqrt{\frac{T}{n}} = \frac{e}{4\pi} (21.691)^{3/2} \beta = 71.43 \beta. \quad (23)$$

Thus we have

$$\frac{l_s}{\bar{d}} = 3.293. \quad (24)$$

Eq. (24) tells us that monopoles and antimonopoles are not far separated on the scale of their screening length. Notice that both of these length scales are much smaller than $|\phi|^{-1}$. However, the impact of all other stable and screened monopoles and antimonopoles on a given stable pair is small due to efficient cancellations of mutual attraction or repulsion. This is expressed by the small lift of the BPS mass $m_{>|\phi|^{-1}}$, compare with Eq. (20).

5 Spatial Wilson loop in effective variables

The effective theory for deconfining SU(2) Yang-Mills theory and the computation of radiative corrections to the pressure is described at length in [5, 8, 14]. We only name those results explicitly that are directly needed and for the remainder refer the reader to these papers.

5.1 Magnetic screening mass

The SU(2) gauge symmetry of the fundamental action is dynamically broken to U(1) by coarse-grained (anti)calorons. Notice that the order parameter ϕ of this gauge-symmetry breaking is determined in a highly nonlocal way [8, 9] thus appealing to the strong magnetic-magnetic correlations mediated by the $|Q| = 1$ (anti)caloron configuration of trivial holonomy [10].

In unitary-Coulomb gauge there are in the effective theory on tree-level one massless vector excitation (hencefore referred to as γ) and two thermal vector quasiparticle excitations (hencefore referred to as V^{\pm}). The transversal γ polarization tensor $\Pi^{\mu\nu}$ is decomposed as

$$\Pi^{\mu\nu} = G(p_0, \mathbf{p}) P_T^{\mu\nu} + F(p_0, \mathbf{p}) P_L^{\mu\nu} \quad (25)$$

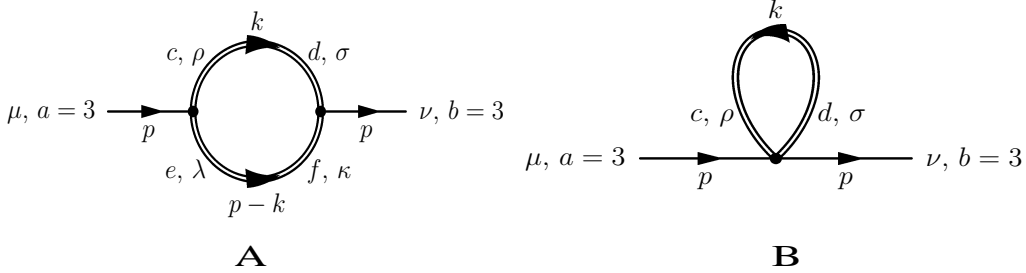


Figure 2: The diagrams for γ 's polarization tensor $\Pi_{\mu\nu}$.

where

$$P_L^{\mu\nu} \equiv \frac{p^\mu p^\nu}{p^2} - g^{\mu\nu} - P_T^{\mu\nu}, \quad (26)$$

and

$$\begin{aligned} P_T^{00} &= P_T^{0i} = P_T^{i0} = 0, \\ P_T^{ij} &= \delta^{ij} - p^i p^j / \mathbf{p}^2. \end{aligned} \quad (27)$$

The functions $G(p_0, \mathbf{p})$ and $F(p_0, \mathbf{p})$ determine the propagation of the interacting γ mode. For $\mu = \nu = 0$ Eq.(25) yields upon rotation to real-time

$$F(p_0, \mathbf{p}) = \left(1 + \frac{p_0^2}{p^2}\right)^{-1} \Pi^{00}. \quad (28)$$

The function $F(p_0, \mathbf{p})$ measures the screening of electric fields which we are not interested in when discussing the *spatial* Wilson loop. For propagation of the γ mode into the 3-direction we have

$$\Pi_{11} = \Pi_{22} = G(p_0, \mathbf{p}). \quad (29)$$

From the magnetic screening function $G(p_0, \mathbf{p})$ we obtain a definition for the magnetic screening m_s as

$$m_s \equiv \lim_{\mathbf{p} \rightarrow 0} \sqrt{\text{Re} G(p_0 = 0, \mathbf{p})}. \quad (30)$$

In Eqs. (29) and (30) we have suppressed the dependence on temperature of the magnetic screening function G . The radiatively generated mass scale m_s measures the exponential decay rate of an externally applied, homogeneous magnetic field $B_i = \epsilon_{ijk} G_{jk}^3$ penetrating the Yang-Mills plasma. In the effective theory, the screening function G only has support for the four-momentum p satisfying the constraint

$$|p^2 - G(p^0, \mathbf{p})| \leq |\phi|^2, \quad (31)$$

where $|\phi|$ is the (temperature-dependent) modulus of the inert, adjoint scalar field ϕ emerging as a consequence of spatial coarse-graining over the stable BPS sector with topological charge modulus $|Q| = 1$. Eq.(31) is the condition that a propagating effective tree-level massless gauge mode in physical Coulomb-unitary gauge must not be further off its radiatively induced mass shell than the scale $|\phi|$ of maximal resolution.

In Fig.2 the two diagrams a priori contributing to $\Pi^{\mu\nu}$ are depicted. Using standard Feynman

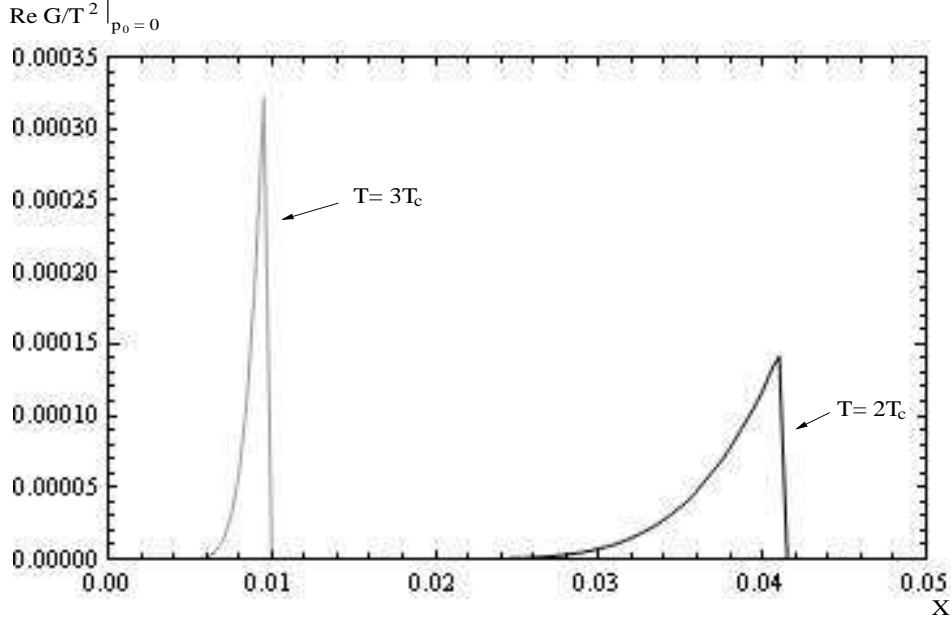


Figure 3: The function $\text{Re } G/T^2$ in dependence of $X = |\mathbf{p}|/T$ setting $p_0 = 0$ for $T = 2T_c$ (black) and $T = 3T_c$ (gray).

rules, we have for diagram A

$$\begin{aligned}
\Pi_A^{\mu\nu}(p) = & \frac{1}{2i} \int \frac{d^4k}{(2\pi)^4} e^2 \epsilon_{ace} [g^{\mu\rho}(-p-k)^\lambda + g^{\rho\lambda}(k-p+k)^\mu + g^{\lambda\mu}(p-k+p)^\rho] \times \\
& \epsilon_{abf} [g^{\sigma\nu}(-k-p)^\kappa + g^{\nu\kappa}(p+p-k)^\sigma + g^{\kappa\sigma}(-p+k+k)^\nu] \times \\
& (-\delta_{cd}) \left(g_{\rho\sigma} - \frac{k_\rho k_\sigma}{m^2} \right) \left[\frac{i}{k^2 - m^2} + 2\pi\delta(k^2 - m^2) n_B(|k_0|/T) \right] \times \\
& (-\delta_{ef}) \left(g_{\lambda\kappa} - \frac{(p-k)_\lambda (p-k)_\kappa}{(p-k)^2} \right) \times \\
& \left[\frac{i}{(p-k)^2 - m^2} + 2\pi\delta((p-k)^2 - m^2) n_B(|p_0 - k_0|/T) \right].
\end{aligned} \tag{32}$$

From the one-loop evolution [5] we know that $e \geq \sqrt{8\pi}$ [8]. Due to constraint $|k^2 - m^2| \leq |\phi|^2$ [5], where $m = 2e|\phi|$, the vacuum part in the V^\pm propagator is forbidden. For an explicit presentation of the γ and V^\pm real-time propagators see Eqs. (36) and (37).

Diagram B reads

$$\begin{aligned}
\Pi_B^{\mu\nu}(p) = & \frac{1}{i} \int \frac{d^4k}{(2\pi)^4} (-\delta_{ab}) \left(g_{\rho\sigma} - \frac{k_\rho k_\sigma}{m^2} \right) \left[\frac{i}{k^2 - m^2} + 2\pi\delta(k^2 - m^2) n_B(|k_0|/T) \right] \times \\
& (-ie^2) [\epsilon_{abe}\epsilon_{cde} (g^{\mu\rho} g^{\nu\sigma} - g^{\mu\sigma} g^{\nu\rho}) + \epsilon_{ace}\epsilon_{bde} (g^{\mu\nu} g^{\rho\sigma} - g^{\mu\sigma} g^{\nu\rho}) + \\
& \epsilon_{ade}\epsilon_{bce} (g^{\mu\nu} g^{\rho\sigma} - g^{\mu\rho} g^{\nu\sigma})].
\end{aligned} \tag{33}$$

Again, the part in Eq. (33) arising from the vacuum contribution in Eq. (36) vanishes. For the four-vertex in diagram B the following constraint holds [5]: $|(p+k)^2| \leq |\phi|^2$.

It is easily seen that only diagram B contributes to m_s . Generalizing $m_s \rightarrow m_s(p_0 = 0, |\mathbf{p}|)$ within the finite support in \mathbf{p} given by the condition (31) now specializing to $|\mathbf{p}^2 + G(p^0 = 0, \mathbf{p})| \leq |\phi|^2$, we obtain a behavior as depicted in Fig. 3 in dependence of $X = |\mathbf{p}|/T$. From Fig. 3 and comparing with Eq. (30) one sees that $m_s = 0$ which is in agreement with our microscopic analysis of Sec. 4. Recall that due to the unresolvability of stable and screened monopole-antimonopole pairs no net monopole or antimonopole density¹⁰ is detected and thus, according to Eq. (23), $l_s \equiv 1/m_s = \infty$.

¹⁰In contrast to Sec. 4.2 we are here concerned with the monopole density as seen in our *effective* theory at resolution $|\phi|$ and not with the hypothetical monopole density detected by a higher resolution.

5.2 Generalities on spatial Wilson loop in effective theory

To compute a Wilson loop in effective variables associated with a given, finite resolution μ is in general something different than the definition in fundamental variables at infinite resolution demands. However, at finite temperature in the deconfining phase of a Yang-Mills theory there is only one resolution scale where the effective action minimally differs from the fundamental action: at $\mu = |\phi|$ technically topologically trivial and nontrivial field configurations are separated modulo mass generation and constraints on the hardness of quantum fluctuations of the former imposed by the latter. Since an ensemble average over isolated and screened magnetic monopoles is generated by the radiative corrections in the effective theory it is suggestive that the spatial Wilson loop evaluated on propagating gauge mode conveying the magnetic flux of the effective theory, with a resummation of the lowest-order radiative effects (polarization tensor) indeed, measures the flux sourced by the ensemble of magnetic monopoles determining the polarization tensor. This argument is purely intuitive, and no proof of this suggested property is yet available.

Here we quote some general results on the calculation of exponentiated one-effective-gauge-boson exchanges within the spatial quadratic contour C of side-length L .

In order to calculate the spatial string tension, we use an expansion into loops for the N -point functions in the effective theory [24]. Because of the rapid numerical convergence of the effective loop expansion [14, 7, 15] we are content here with a resummation of the one-loop polarization tensor for the γ mode into its effective propagator and the tree-level propagator for the V^\pm modes (2-point functions). The exchange of these modes is subsequently exponentiated in order to take into account higher N -point functions in a trivial way, see Fig. 4.

Thus we can write for the logarithm of $W[C]$

$$\ln W[C] = -\frac{1}{2}C_F \oint dx_\mu dy_\nu D_{\mu\nu}(x-y), \quad (34)$$

where C_F denotes the Dynkin index in the fundamental representation, defined as the normalization factor of the generators of the algebra (i.e. $C_F \equiv \frac{1}{2}$), and

$$D_{\mu\nu} = \sum_{a=1}^3 D_{\mu\nu}^{(a)} \quad (35)$$

is the sum of the tree-level propagators (V^\pm corresponds to $a = 1, 2$) and the one-loop resummed propagator (γ corresponds to $a = 3$).

The tree-level propagators for $a = 1, 2$ in position space are given as the Fourier transformations of their momentum space counterparts

$$D_{\mu\nu}^{1,2}(\beta, x-y) = - \int \frac{d^4 p}{(2\pi)^4} e^{-ip(x-y)} \left(g_{\mu\nu} - \frac{p_\mu p_\nu}{m^2} \right) \left[\frac{i}{p^2 - m^2 + i\varepsilon} + 2\pi\delta(p^2 - m^2)n_B(\beta|p_0|) \right]. \quad (36)$$

The one-loop resummation of the magnetic part¹¹ of the polarization tensor (screening function G) into the dressed γ propagator, see Eq. 25, yields the following result

$$D_{\mu\nu}^3(\beta, x-y) = \int \frac{d^4 p}{(2\pi)^4} e^{-ip(x-y)} \left[P_{\mu\nu}^T \left(\frac{i}{p^2 - G(p^0, \mathbf{p}) + i\varepsilon} + 2\pi\delta(p^2 - G(p^0, \mathbf{p}))n_B(\beta|p_0|) \right) - i \frac{u_\mu u_\nu}{\mathbf{p}^2} \right], \quad (37)$$

where the transversal projection operator is given as

$$\begin{aligned} P_{00}^T(p) &= P_{0i}^T(p) = P_{i0}^T(p) = 0 \\ P_{ij}^T(p) &= \delta_{ij} - \frac{p_i p_j}{\mathbf{p}^2}. \end{aligned} \quad (38)$$

¹¹We are not interested in electric screening effects since we study the *spatial* Wilson loop.

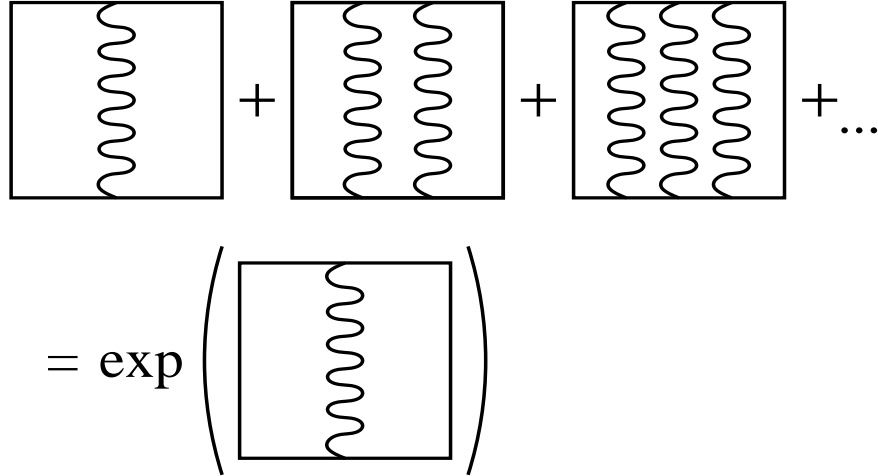


Figure 4: Illustration of the diagrammatic approach. Every summand in this formula represents a whole class of N -gauge-boson exchange diagrams, which is encoded in terms of a (suppressed) combinatoric factor.

We calculate the contour integral in the 1-2-plane, that is $x_0 = y_0 = x_3 = y_3 = 0$, and consider at first an arbitrary propagator $D_{\mu\nu}(p)$. Later we will insert the explicit expressions for $D_{\mu\nu}^{1,2}$ (V^\pm gauge modes) and for $D_{\mu\nu}^3$ (γ mode). We obtain [25]

$$\begin{aligned} \ln W[C] &= -\frac{1}{4} \int \frac{d^4 p}{(2\pi)^4} \oint \oint dx_\mu dy_\nu D_{\mu\nu}(p) e^{-ip(x-y)} \Big|_{x_0=y_0=x_3=y_3=0} \\ &= -4 \int \frac{d^4 p}{(2\pi)^4} \sin^2\left(\frac{p_1 L}{2}\right) \sin^2\left(\frac{p_2 L}{2}\right) \left(\frac{D_{11}}{p_1^2} - \frac{D_{12}}{p_1 p_2} - \frac{D_{21}}{p_1 p_2} + \frac{D_{22}}{p_2^2} \right). \end{aligned} \quad (39)$$

5.3 Thermal part due to massive modes

Here we present the result for the contribution of the (thermal part of) the V^\pm propagators to the logarithm of the spatial Wilson loop. Inserting the thermal part of the V^\pm propagator in Eq. (36) into Eq. (39), we have

$$\ln W[C]_{V^\pm} = \frac{1}{\pi^3} \int d^3 p \frac{\sin^2\left(\frac{p_1 L}{2}\right) \sin^2\left(\frac{p_2 L}{2}\right)}{\sqrt{p_1^2 + p_2^2 + p_3^2 + m^2}} n_B(\beta \sqrt{p_1^2 + p_2^2 + p_3^2 + m^2}) \left(\frac{1}{p_1^2} + \frac{1}{p_2^2} \right). \quad (40)$$

Let us now rescale the momenta p_i and the squared V^\pm mass m^2 in Eq. (40) to dimensionless variables as follows

$$\hat{p}_i = p_i \cdot L, \quad (41)$$

and using $e = \sqrt{8\pi}$,

$$\hat{m}^2 = \frac{m^2}{T^2} = \frac{(2e)^2}{T^2} \frac{\Lambda}{2\pi T} = \frac{128\pi^4}{\lambda^3}, \quad (42)$$

where L is the side-length of the spatial quadratic contour C . To eventually perform the limit $L \rightarrow \infty$, we introduce the dimensionless parameter τ as

$$\tau = T \cdot L. \quad (43)$$

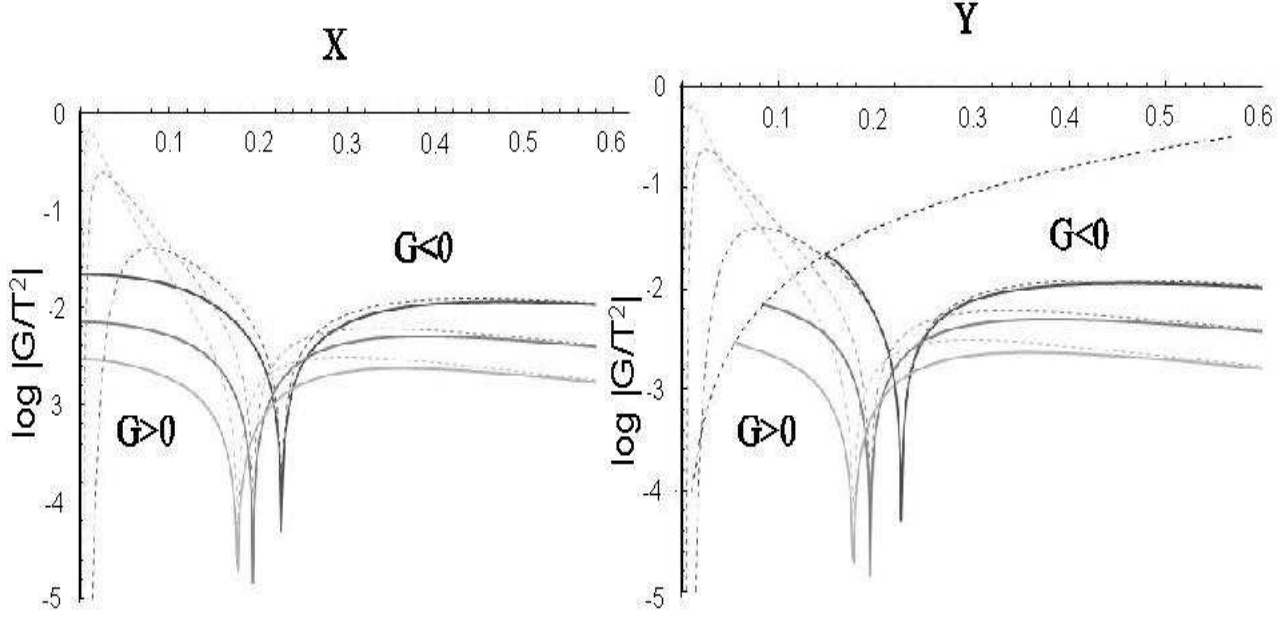


Figure 5: Plots of $\log \left| \frac{G}{T^2} \right|$ in the full calculation (solid grey curves) and for the approximation $p^2 = 0$ (dashed grey curves). The cusps in $\log \left| \frac{G}{T^2} \right|$ correspond to zeros separating the regime of screening ($G > 0$) from the regime of antiscreening ($G < 0$). The left panel depicts $\log \left| \frac{G}{T^2} \right|$ as a function of X . The right panel shows $\log \left| \frac{G}{T^2} \right|$ as a function of $Y \equiv \sqrt{X^2 + \frac{G}{T^2}}$. Here the dashed black curve is the function $2 \log Y$. In order of increasing lightness the curves correspond to $T = 2T_c$, $T = 3T_c$, and $T = 4T_c$.

Eq. (40) is then recast as

$$\ln W[C]_{V^\pm} = \frac{1}{\pi^3} \int d\hat{p}_1 d\hat{p}_2 d\hat{p}_3 \frac{\sin^2 \left(\frac{\hat{p}_1}{2} \right) \sin^2 \left(\frac{\hat{p}_2}{2} \right)}{\sqrt{\hat{p}_1^2 + \hat{p}_2^2 + \hat{p}_3^2 + \frac{128\pi^4}{\lambda^3} \tau^2}} n_B \left(\frac{\sqrt{\hat{p}_1^2 + \hat{p}_2^2 + \hat{p}_3^2 + \frac{128\pi^4}{\lambda^3} \tau^2}}{\tau} \right) \left(\frac{1}{\hat{p}_1^2} + \frac{1}{\hat{p}_2^2} \right). \quad (44)$$

From Eq. (44) it is obvious that in the limit $\tau \rightarrow \infty$ the contribution to $\frac{\ln W[C]}{\tau^2}$ of the V^\pm modes is nil, and we no longer need to discuss their potential impact on the spatial string tension.

5.4 Thermal part due to massless mode

Let us now discuss the contribution of the thermal part of the γ mode to $\ln W[C]$. In [18] we have computed the screening function G selfconsistently on the radiatively induced mass shell $p^2 - G(p^0, \mathbf{p}) = 0$. On this mass-shell, only diagram B in Fig. 2 contributes. In Fig. 5 the dependence of $\log \left| \frac{G}{T^2} \right|$ on the dimensionless spatial momentum modulus $X \equiv \frac{|\mathbf{p}|}{T}$ (left-panel) and on dimensionless frequency $Y = \sqrt{X^2 + \frac{G}{T^2}}$ (right-panel) is depicted for various temperatures. Inserting the thermal part of the magnetically dressed γ propagator of Eq. (37) into Eq. (39), we obtain

$$\ln W[C]_\gamma^{\text{th}} = -\frac{1}{2\pi^3} \int d\hat{p}_1 d\hat{p}_2 d\hat{p}_3 \frac{\sin^2 \left(\frac{\hat{p}_1}{2} \right) \sin^2 \left(\frac{\hat{p}_2}{2} \right)}{\sqrt{\hat{p}_1^2 + \hat{p}_2^2 + \hat{p}_3^2 + \hat{G}\tau^2}} n_B \left(\frac{\sqrt{\hat{p}_1^2 + \hat{p}_2^2 + \hat{p}_3^2 + \hat{G}\tau^2}}{\tau} \right) \left(\frac{1}{\hat{p}_1^2} + \frac{1}{\hat{p}_2^2} \right), \quad (45)$$

where $\hat{G} \equiv \frac{G}{T^2}$. In Fig. 6 plots of $-\ln W[C]_\gamma^{\text{th}}$ for $T = 2T_c, 3T_c$, and $4T_c$ are shown as functions of τ . Clearly, for each temperature and for large τ we observe a *perimeter* law in the approximation

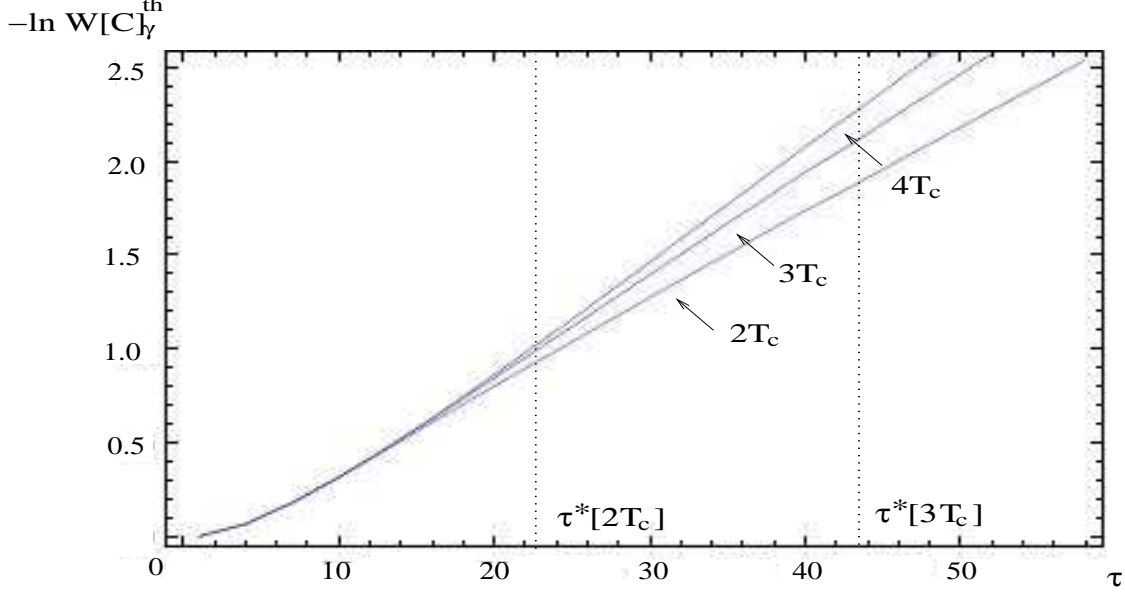


Figure 6: Plots of $-\ln W[C]_\gamma^{\text{th}}$ as a function of $\tau = T \cdot L$. The dotted lines correspond to the value of L coinciding with the minimal length scale $|\phi|^{-1}$ in the effective theory at a given temperature. The left line is for $T = 2T_c$, the right line for $T = 3T_c$, and the line for $T = 4T_c$ would be at $\tau^*[4T_c] = 65.77$ and thus is not contained in the figure.

used¹². For τ considerably below τ^* , which is associated with the maximal resolution $|\phi|$ (we set $L = |\phi|^{-1}$ in Eq. (43)), we do, however, observe curvature in $-\ln W[C]_\gamma^{\text{th}}$.

5.5 Quantum part due to massless mode

We now turn to the contribution to $\ln W[C]_\gamma$ of the quantum part of γ 's dressed propagator. Inserting the quantum part of the magnetically dressed γ propagator of Eq. (37) into Eq. (39), we obtain

$$\ln W[C]_\gamma^{\text{vac}} = -\frac{i}{4\pi^4} \int d^4 \hat{p} \sin^2\left(\frac{\hat{p}_1}{2}\right) \sin^2\left(\frac{\hat{p}_2}{2}\right) \frac{1}{\hat{p}^2 - \hat{G}\tau^2 + i\epsilon} \left(\frac{1}{\hat{p}_1^2} + \frac{1}{\hat{p}_2^2}\right), \quad (46)$$

where $\hat{G} \equiv \frac{G}{T^2}$ and $\hat{p}_0 \equiv p_0 L$. Notice that in this case the screening function G receives contributions from both diagrams A and B in Fig. 2 because the only constraint on γ 's momentum is $|p^2 - \text{Re} G(p^0, \mathbf{p})| \leq |\phi|^2$. In Fig. 7 the imaginary part of G (due to diagram A) is plotted as a function of $X_0 \equiv \frac{p_0}{T}$ and of $X \equiv \frac{\mathbf{p}}{T}$ at $T = 2T_c$. Clearly, $\text{Im} G$ is nonvanishing only within a small region centered at the origin of the $X_0 - X$ plane. Fig. 7 suggests that the modulus of the factor $\frac{1}{\hat{p}^2 - \hat{G}\tau^2 + i\epsilon}$ in Eq. (46) can be estimated by the situation of unadulterated γ propagation. That is, we approximately may evaluate the integral in Eq. (46) by setting $G = 0$. To do this, one may imagine the condition $|p^2| \leq |\phi|^2$ to be implemented in such a way that a strongly-decaying analytic factor (for $|p^2| > |\phi|^2$), is introduced to make the use of the theorem of residues applicable. One then obtains

$$\ln W[C]_\gamma^{\text{vac}} = \frac{1}{2\pi^3} \int d^3 \hat{p} \sin^2\left(\frac{\hat{p}_1}{2}\right) \sin^2\left(\frac{\hat{p}_2}{2}\right) \frac{1}{\sqrt{\hat{p}_1^2 + \hat{p}_2^2 + \hat{p}_3^2}} \left(\frac{1}{\hat{p}_1^2} + \frac{1}{\hat{p}_2^2}\right). \quad (47)$$

¹²Again, we believe that this approximation captures all the essential physics due to the rapid convergence in the number of external legs in N -point functions. Notice that in a one-loop diagram making up a radiative correction to γ 's N -point function there are $N - 1$ independent external four momenta p_i all of which are subject to the constraint $|p_i^2| \leq |\phi|^2$. With increasing N this should rapidly suppress the contribution of one-loop corrections to γ 's N -point function. Moreover, the expansion into the number M of loops at a given N does converge rapidly [7, 14, 15].

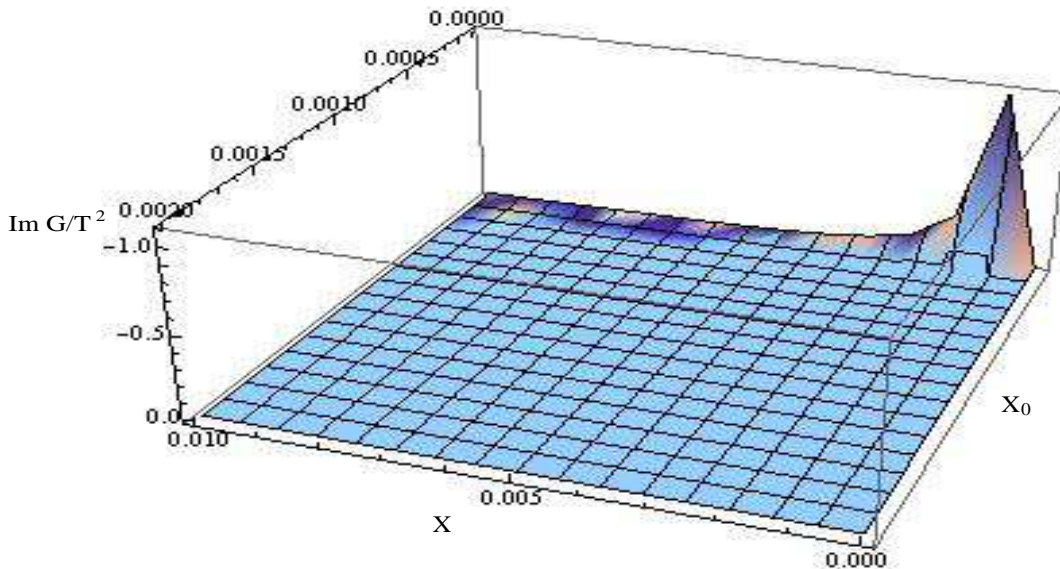


Figure 7: $\text{Im } G/T^2$, as originating from diagram A in Fig. 2, as a function of $X_0 \equiv \frac{p_0}{T}$ and of $X \equiv \frac{p}{T}$ at $T = 2T_c$

The integral in Eq.(47) is UV divergent. Introducing a UV cutoff, one sees that the part of the spectrum, where $G > 0$, contributes a real monotonic-decreasing-in- τ function whereas for $G < 0$ and sufficiently large τ the contribution is imaginary with modulus that is also a monotonic-decreasing-in- τ function. Furthermore the UV divergence itself does not depend on τ . Thus we may refrain from considering this quantum contribution any further.

5.6 Summary of results obtained in effective variables

To summarize, the only nontrivial contribution to $\ln W[C]_\gamma$ arises from the thermal part of the resummed γ -propagator as investigated in Sec.5.4. There we observe that for hypothetic values of L smaller than the minimal length $|\phi|^{-1}$ in the effective theory an area law emerges. This is qualitatively in line with lattice investigations using the Wilson action at finite lattice spacing, see Sec.6, in the sense that an artificial resolution scale is introduced to probe the system at small spatial distances.

6 Conclusions

For the deconfining phase of SU(2) Yang-Mills thermodynamics we have argued that there is a unique effective action emerging when applying a combination of spatial-coarse graining and separation of BPS saturated field configurations from trivial-topology fluctuations. This programme essentially appeals to spatial homogeneity and isotropy of thermodynamical systems, the perturbative renormalizability of the theory [17], and the fact that fundamental as well as effective BPS configurations possess no energy-stress and thus do not propagate.

Subsequently, we have investigated the physics of screened magnetic (anti)monopoles, as they emerge by the dissociation of large-holonomy (anti)calorons, both in a hypothetic setting assuming a larger resolution than the maximal resolution of the effective theory for the deconfining phase $|\phi|$ [8] and in terms of the spatial Wilson loop computed in effective variables. While the former investigation is safe since radiative corrections [7, 14] are under accurate control¹³ in the effective theory, the latter approach assumes that the physical content of the definition of the Wilson loop

¹³There are kinematic constraints on the propagation of effective fields as imposed by the thermal ground state:

in fundamental field variables, which is modulo certain approximations (see below) employed in direct lattice computations, is the same as the definition in terms of thermal-ground-state influenced propagating, effective field variables. Although it is suggestive that this is true, we so far have no proof for this correspondence. So this question remains open. At the same time, however, the computation of the mean density of screened and stable monopole-antimonopole pairs from an energy-density deficit introduced by a certain effective two-loop correction to the pressure [14] as compared to the free quasiparticle situation and the subsequent calculation of the magnetic screening length implies that according to the interpretation of Ref. [20] no area law can arise as a consequence of the magnetic flux of a given pair decaying too rapidly. This is also what the computation of the effective Wilson loop indicates.

Therefore, our results using these two alternative methods match in the sense that there is no area-law for the effective spatial Wilson loop at a fixed temperature and in the limit of large contour size although an area law emerges in the direct calculation of the Wilson loop in the effective theory when the contour size falls below the resolution $|\phi|$ which, of course, is an unphysical situation.

In lattice simulations the typical spatial resolution – the inverse spatial lattice spacing – even at temperatures a few times T_c is considerably larger than the natural¹⁴ resolution $|\phi|$ of continuum and infinite-volume Yang-Mills thermodynamics [2, 3]. Lattice simulations are usually performed with the Wilson action at *finite* values of the lattice spacing a . However, due to the contribution of topologically nontrivial field configurations to the partition function a renormalization-group evolved perfect lattice action certainly is more complicated than the Wilson action obtained from the continuum Yang-Mills action by naive discretization. Using the Wilson action, the scaling regime for the fundamental coupling hardly makes any reference to bulk properties of the highly nonperturbative ground-state physics (trace anomaly [21]). So what we have indirectly argued for in this work is that the physics of screened and isolated magnetic (anti)monopoles is very sensitive to a mild resolution dependence of the *partition function* as it is artificially introduced by the Wilson action. In principle, this action should be modified by nonperturbative effects yielding the perfect lattice action. The latter, however, is extremely hard to generate at finite temperatures.

Given this observation and the principle problem of comparison between fundamental Wilson loop and its effective counterpart it is not surprising that an area law for the spatial Wilson loop is measured in lattice simulations (in accord with a 3D strong-‘coupling’-expansion argument [1]) subject to the Wilson action. Notice that the introduction of a finite spatial lattice spacing still working with the Wilson action actually acts physically (which it should not) in separating monopoles from antimonopoles. As a result, a net magnetic flux is measured through the spatial contour in lattice simulations although it is not clear in what sense the nonabelian flux through the Wilson loop defined in fundamental variables is related to the abelian flux that we investigate by the γ mode’s contribution to the effective Wilson loop. We stress that lattice simulations using the Wilson action are interesting and important because they strongly point to certain aspects of the highly nonperturbative ground-state physics. However, we suspect that they are not sufficiently adapted to describe the subtle effects attributed to large-holonomy (anti)caloron dissociation as they take place in infinite-volume continuum Yang-Mills thermodynamics. To turn this into a completely rigorous statement for the Wilson loop in effective variables the above-mentioned correspondence would have to be proved, and a precise estimate for the contribution to the integration over the spatial contour of N -point functions with higher internal loop number would have to be obtained. We leave this to future investigation.

Maximal offshellness and maximal momentum transfer in a local vertex. Using the Euler-L’Huillier characteristics for spherical polyhedra (including a nontrivial genus) one shows that increasing the number of vertices in irreducible loop diagrams the number of constraints on a priori noncompact integration variables rapidly exceeds the number of variables. This suggests a termination of the expansion in irreducible loop diagrams at a finite loop order. Example calculation for the pressure up to three loops [14, 15] provide ample evidence for this conjecture.

¹⁴By ‘natural’ we mean that at maximal resolution $|\phi|$ the effective action for deconfining Yang-Mills thermodynamics is of the simple form of Eq. (1).

Acknowledgments

We would like to thank Markus Schwarz for very useful conversations and helpful comments on the manuscript. A Referee's helpful queries are gratefully acknowledged.

References

- [1] C. Borgs, Nucl. Phys. B **261**, 455 (1985).
- [2] E. Manousakis and J. Polonyi, Phys. Rev. Lett. **58**, 847 (1987).
- [3] G. S. Bali et al., Phys. Rev. Lett. **71**, 3059 (1993).
- [4] M. Laine and Y. Schröder, JHEP **0503** 067 (2005) and references therein.
- [5] R. Hofmann, Int. J. Mod. Phys. A**20** (2005) 4123, Erratum-ibid. A **21** (2006) 6515.
R. Hofmann, Mod. Phys. Lett. A**21**, 999 (2006), Erratum-ibid. A **21**, 3049 (2006).
- [6] F. Giacosa and R. Hofmann, Prog. Theor. Phys. **118**, 759 (2007) [hep-th/0609172].
- [7] R. Hofmann, hep-th/0609033.
- [8] R. Hofmann, arXiv:0710.0962 [hep-th].
- [9] U. Herbst and R. Hofmann, hep-th/0411214.
- [10] B. J. Harrington and H. K. Shepard, Phys. Rev. D **17**, 2122 (1978).
- [11] W. Nahm, Phys. Lett. B **90**, 413 (1980).
W. Nahm, *Selfdual Monopoles and Calorons*. Lect. Notes in Physics. 201, eds. G. Denaro, e.a. (1984) p. 189, Springer Berlin-Heidelberg-New York.
K.-M. Lee and C.-H. Lu, Phys. Rev. D **58**, 025011 (1998).
T. C. Kraan and P. van Baal, Phys. Lett. B **428**, 268 (1998).
T. C. Kraan and P. van Baal, Phys. Lett. B **435**, 389 (1998).
- [12] D. J. Gross, R. D. Pisarski, and L. G. Yaffe, Rev. Mod. Phys. **53**, 43 (1981).
- [13] T. W. B. Kibble, *J. Phys. A*, **9** 1387 (1976).
- [14] M. Schwarz, R. Hofmann and F. Giacosa, Int. J. Mod. Phys. A **22**, 1213 (2007).
- [15] D. Kaviani and R. Hofmann, Mod. Phys. Lett. A **22**, 2343 (2007).
- [16] J. Keller, R. Hofmann, and F. Giacosa, Int. J. Mod. Phys. A **23**, 5181 (2008).
- [17] G. 't Hooft and M. J. G. Veltman, Nucl. Phys. B **44**, 189 (1972).
G. 't Hooft, Nucl. Phys. B **33**, 173 (1971).
G. 't Hooft, Nucl. Phys. B **62**, 444 (1973).
G. 't Hooft and M. J. G. Veltman, Nucl. Phys. B **50**, 318 (1972).
B. W. Lee and Jean Zinn-Justin, Phys. Rev. D **5**, 3121 (1972).
B. W. Lee and Jean Zinn-Justin, Phys. Rev. D **5**, 3137 (1972).
B. W. Lee and Jean Zinn-Justin, Phys. Rev. D **5**, 3155 (1972).
- [18] J. Ludescher and R. Hofmann, Ann. Phys.**18**, 271 (2009) [arXiv:0806.0972 [hep-th]].

- [19] A. M. Polyakov, Phys. Lett. B **59**, 82 (1975).
C. P. Korthals Altes, hep-ph/0408301.
C. P. Korthals Altes, Acta Phys. Polon. B **34**, 5825 (2003).
P. Giovannangeli and C. P. Korthals Altes, Nucl. Phys. B **608**, 203 (2001).
C. Korthals-Altes, A. Kovner, and M. A. Stephanov, Phys. Lett. B **469**, 205 (1999).
- [20] C. Korthals-Altes, hep-ph/0406138v2.
- [21] F. Giacosa and R. Hofmann, Phys. Rev. D **76**, 085022 (2007). [hep-th/0703127]
- [22] D. Diakonov, N. Gromov, V. Petrov, S. Slizovskiy, Phys. Rev. D **70**, 036003 (2004). [hep-th/0404042]
- [23] U. Herbst, R. Hofmann, J. Rohrer, Acta Phys. Pol. **B36**, 881 (2005).
- [24] A. Bassetto, G. Nardelli, and R. Soldati, *Yang-Mills Theories in Algebraic Non-Covariant Gauges: Canonical Quantization and Renormalization*, World Scientific Publishing Company (1991), Singapore.
- [25] J. Keller, Diploma thesis Universität Heidelberg, arXiv:0801.3961.

This figure "Fig-3bi.jpg" is available in "jpg" format from:

<http://arxiv.org/ps/0812.1858v4>